Hydrol. Earth Syst. Sci. Discuss., 6, 6759–6793, 2009
www.hydrol-earth-syst-sci-discuss.net/6/6759/2009/

Hydrology and Earth System Sciences Discussions

This discussion paper is/has been under review for the journal Hydrology and Earth System Sciences (HESS). Please refer to the corresponding final paper in HESS if available.

CFD modelling approach for dam break flow studies

C. Biscarini[1,3], S. Di Francesco[2,3], and P. Manciola[2]

[1]Water Resources Research And Documentation Centre, University For Foreigners, Villa La Colombella, 0634 Perugia, Italy
[2]Department of Civil and Environmental Engineering, University of Perugia, Via G. Duranti 93, 06125 Perugia, Italy
[3]H[2]CU, Honors Center of Italian Universities, University of Rome La Sapienza, Rome, Italy

Received: 5 October 2009 – Accepted: 13 October 2009 – Published: 3 November 2009

Correspondence to: C. Biscarini (biscarini.chiara@unistrapg.it)

Published by Copernicus Publications on behalf of the European Geosciences Union.

Abstract

This paper presents numerical simulations of free surface flows induced by a dam break comparing the shallow water approach to fully three-dimensional simulations. The latter are based on the solution of the complete set of Reynolds-Averaged Navier-Stokes (RANS) equations coupled to the Volume of Fluid (VOF) method.

The methods assessment and comparison are carried out on a dam break over a flat bed without friction and a dam break over a triangular bottom sill. Experimental and numerical literature data are compared to present results.

The results demonstrate that the shallow water approach loses some three-dimensional phenomena, which may have a great impact when evaluating the downstream wave propagation. In particular, water wave celerity and water depth profiles could be underestimated due to the incorrect shallow water idealization that neglects the three-dimensional aspects due to the gravity force, especially during the first time steps of the motion.

1 Introduction

A dam break is the partial or catastrophic failure of a dam which leads to an uncontrolled release of water. The potential catastrophic failure and the resultant downstream flood damage is a scenario that is of great concern.

The mitigation of the impacts to the greatest possible degree requires modelling of the flood with sufficient detail so as to capture both the spatial and temporal evolutions of the flood event (Jorgenson et al., 2004). The selection of an appropriate model to correctly simulate dambreak flood routing is therefore an essential step.

Traditionally, one-dimensional models have been used to model dam break flooding, but these models are limited in their ability to capture the flood spatial extent, in terms of flow depth and velocity and timing of flood arrival and recession, with any degree of detail.

The development in the last years has led to several numerical models aimed at solving the so-called dam break problem (Soarez Frazao, 2002).

The Concerted Action on Dam Break Modelling (CADAM) project (Morris and Galland, 1998), has been set in motion by the European Union to investigate current methods and use in simulating and predicting the effects of dam failures. The obtained results show that shallow water scheme is reasonably suitable for the representation of free surface sharp transient (Wang et al., 2000). The authors concluded that shallow water methods agree satisfactorily with experimental results (Alcrudo and Garcia-Navarro, 1998).

However, in some cases, these mathematical models and numerical solvers do not seem adequate to simulate some observed hydraulic aspects. For instance, the wave front celerity may be underestimated and water depth profiles are not well reproduced. In the short time step immediately after the gate collapse, in fact, the flow is mainly influenced by vertical acceleration due to gravity and gradually-varied flow hypothesis does not hold. To emphasize these effects, three-dimensional numerical simulations have been carried out by Manciola et al. (1994) and De Maio et al. (2004).

The recent advances in computer software and hardware technology have led to the development and application of three-dimensional Computational Fluid Dynamics (CFD) models, based on the complete set of the Navier Stokes equations, also to typical hydraulic engineering case, as flow over weirs, through bridge piers and dam breaks (Mohammadi, 2008; Nagata et al., 2005).

To validate numerical simulations of flooding waves and to investigate current methods and their use in simulating and predicting the effects of dam failures, the CADAM has defined a set of analytical and experimental benchmarks. In the present paper the validation proposed by CADAM is applied and two test cases are considered:

- a dam break over a dry bed without friction (Fennema and Chaundry, 1990);
- a dam break over a triangular bottom sill (Soarez, 2002).

We compare the experimental data with the modelling results deriving from a shallow water and a detailed Navier-Stokes numerical models. The former is based on two-dimensional hydrodynamics and sediment transport model for unsteady open channel flows and the latter on Reynolds-averaged Navier-Stokes algorithm. In the latter, the water-air interface is captured with the volume of fluid (VOF) method.

2 Numerical modelling

Using an Eulerian approach, the description of fluid motion requires that the thermodynamic state be determined in terms of sensible fluid properties, pressure, P, density, ρ and temperature, T, and of the velocity field $\vec{V}(\vec{x},t)$ (Hirsch, 1992; Abbott and Basco, 1989; Patankar, 1981).

Therefore, in a three-dimensional space for a given fluid system having two intensive degrees of freedom, we have six independent variables as unknowns, thus requiring six independent equations. The six equations (Navier-Stokes equations) are given by the equation of state and the three fundamental principles of conservation:

- Mass continuity

$$\frac{\partial \rho}{\partial t} + \vec{u} \cdot \vec{\nabla} \rho = 0 \tag{1}$$

  where ρ is the fluid density;

- Newton 2nd law or momentum conservation that leads to the well known Navier-Stokes system of equations (three equations in a three-dimensional space x, y and z)

$$\frac{\partial \rho \vec{V}}{\partial t} + \vec{\nabla}(\rho \vec{V} \vec{V}) = -\vec{\nabla} p + \rho \vec{f} + \frac{\mu}{3} \vec{\nabla}(\nabla \vec{V}) + \mu \nabla^2 \vec{V} \tag{2}$$

where $\vec{f}$ is a specific prescribed body force (i.e. gravity force) and μ is the fluid dynamic viscosity;

– Energy conservation (1st law of thermodynamics);

For the majority of hydraulic applications involving water flow, however, some simplifications are always present, as:

– the fluid flow is considered isothermal and the energy conservation equation simply becomes $dT=0$;

– the fluid flow can be considered incompressible.

Therefore, the most general macroscopic model for hydraulic flows may be represented by the incompressible Navier-Stokes equations:

$$\rho\left(\frac{\partial\vec{V}}{\partial t}-\vec{f}\right)=-\vec{\nabla}p+\mu\nabla^2\vec{V} \tag{3}$$

The above system of equations, however, is valid for one phase, while in hydraulic flows at least two phases are always present, water and air. The task of simulating the behaviour of multi-phase flows is very challenging, due to the inherent complexity of the involved phenomena (i.e. moving interfaces with complex topology), and represents one of the leading edges of computational physics.

Different approaches have been developed to track the water-air interface in hydraulic problems. In this paper we compare the detailed NS model coupled to the VOF approximation with the simplified shallow water model that, as a matter of fact, leaves the multiphase nature of hydraulic flows by simulating the fluid dynamics in two dimensions and assuming a simplified approach for the water elevation dimension.

2.1 Turbulence modelling

In principle, Navier-Stokes equation can be used to simulate both laminar and turbulent flows without averaging or approximations other than the necessary numerical

discretisations. However, turbulent flows at realistic Reynolds numbers span a large range of turbulent length and time scales and in a Direct Numerical Simulation (DNS) the discretisation of the domain should capture all of the kinetic energy dissipation, thus involving length scales that would require a prohibitively fine mesh for practical engineering problems (the total cost of a direct simulation is proportional to Re^3).

A large amount of CFD research has concentrated on methods which make use of turbulence models to predict the effects of turbulence in fluid flows without resolving all scales of the smallest turbulent fluctuations. There are two main groups of turbulence models:

– the introduction of averaged and fluctuating quantities that modify the unsteady Navier-Stokes into the Reynolds Averaged Navier-Stokes (RANS) equations (Rodi, 1980);

– Large Eddy Simulation (LES) (Galperin and Orszag, 1993) approach based on the filtering of the flow field by directly simulating the large-scale structures (resolved grid scales), which are responsible for most of the transport of mass and momentum, and somehow modelling the small-scale structures (unresolved subgrid scales), the contribution of which to momentum transport is little.

In this paper the RNG k-ε model is used in both the shallow water approximation and the detailed three-dimensional simulation.

The computational effort required by the LES models, often used as an intermediate technique between the DNS of turbulent flows and the resolution of RANS equations, are in fact unacceptable for large-scale problems, as the one presented in this paper.

2.2 Two-dimensional shallow water numerical model

The shallow water model (Faber, 1995) approximation is based on the hypothesis that a layer of water flows over a horizontal, flat surface with elevation $Z\,(x,y,t)$. This means that the pressure distribution along each vertical is hydrostatic. If we assume that the

horizontal scale of flow features is large compared to the depth of the water, the flow velocity is independent of depth (i.e. $v=v(x,y,t)$) and that the water within the layer is in hydrostatic balance, the model equations become:

$$\text{Continuity Equation}: \quad \frac{\partial Z}{\partial t} + \frac{\partial (hU)}{\partial x} + \frac{\partial (hV)}{\partial y} = 0 \tag{4}$$

Momentum Equations:

$$\begin{aligned} \frac{\partial u}{\partial t} + u\frac{\partial u}{\partial x} + v\frac{\partial u}{\partial y} &= -g\frac{\partial Z}{\partial x} + \frac{1}{h}\left[\frac{\partial (h\tau_{xx})}{\partial x} + \frac{\partial (h\tau_{yx})}{\partial y}\right] - \frac{\tau_{bx}}{\rho h} + f_{\text{Cor}} v \\ \frac{\partial v}{\partial t} + u\frac{\partial v}{\partial x} + v\frac{\partial v}{\partial y} &= -g\frac{\partial Z}{\partial y} + \frac{1}{h}\left[\frac{\partial (h\tau_{yx})}{\partial x} + \frac{\partial (h\tau_{yy})}{\partial y}\right] - \frac{\tau_{by}}{\rho h} + f_{\text{Cor}} u \end{aligned} \tag{5}$$

where u and v are the depth-integrated velocity components in the x and y directions respectively; g is the gravitational acceleration; Z is the water surface elevation; ρ is water density; h is the local water depth; f_{Cor} is the Coriolis parameter; τ_{yx}, τ_{xx}, τ_{yy}, are the depth integrated Reynolds stresses; and τ_{bx} and τ_{by} are the shear stresses on the bed surface.

The above system of equations basically results from a depth averaging procedure of the Navier-Stokes equations and is usually called depth integrated two-dimensional Navier-Stokes equations (or Shallow Water model). As a matter of fact, the shallow water model is a single phase model, as only the water flow field in the plane x-y is solved.

2.3 Numerical scheme for the shallow water approach

In this paper, the shallow water approach is tested by using the open-source CCHE2D code, developed at the National Center for Computational Hydroscience and Engineering (NCCHE), University of Mississippi (Jia and Wang, 1999). This code has been extensively developed, verified, refined, validated, documented and applied to simulate a variety of free surface flow and sediment transport related phenomena (Jia and Wang, 2001).

Boussineq's theory (Boussinesq, 1903) is used to approximate turbulent shear stresses and the standard k-ε model is employed to simulate the two test cases (Rodi, 1980).

The set of SW equations is solved implicitly using the control volume approach and the efficient element method (Wang and Hu, 1992). The continuity equation for surface elevation is solved on a structured grid with quadrilateral elements. At each node an element is formed using the surrounding eight nodes making a total of nine nodes working element. In addition the depth-integrated k-ε model is implemented and included in the code. (Jia and Wang, 1999, 2001).

2.4 Three-dimensional multiphase model

The three-dimensional multiphase approach is based on the numerical resolution of the incompressible Navier-Stokes equations. To maintain the multiphase nature of the flow, there are currently two approaches widely used: the Euler-Lagrange approach and the Euler-Euler approach. In the latter approach, the different phase is taken into account by considering that the volume of a phase cannot be occupied by other phases. Then the concept of phase volume fractions as continuous functions of space and time is introduced.

In this paper, the so-called Volume Of Fluid (VOF) method is used. The VOF method is a surface-tracking technique applied to a fixed Eulerian mesh, in which a specie transport equation is used to determine the relative volume fraction of the two phases, or phase fraction, in each computational cell. Practically, a single set of Reynolds-averaged Navier-Stokes equations is solved and shared by the fluids and for the additional phase, its volume fraction γ is tracked throughout the domain.

Therefore, the full set of governing equations for the fluid flow are:

$$\nabla \cdot \boldsymbol{u} = 0 \tag{6}$$

$$\frac{\partial \rho \boldsymbol{u}}{\partial t} + \nabla \cdot (\rho \boldsymbol{u}\boldsymbol{u}) - \nabla \cdot ((\mu + \mu_t)S) = -\nabla p + \rho g + \sigma K \frac{\nabla \gamma}{|\nabla \gamma|} \tag{7}$$

$$\frac{\partial \gamma}{\partial t} + \nabla \cdot (\boldsymbol{u}\gamma) = 0 \tag{8}$$

where $\boldsymbol{u}$ is the velocity vector field, p is the pressure field, μ_t is the turbulent eddy viscosity, S is the strain rate tensor defined by $S = \frac{1}{2}(\nabla \boldsymbol{u} + \nabla \boldsymbol{u}^T)$, σ is the surface tension and K is the surface curvature.

For the incompressible phase volume fraction, γ, the following three conditions are possible:

- $0<\gamma<1$: when the infinitesimal volume contains the interface between the q-th fluid and one or more other fluids;
- $\gamma = 0$: volume occupied by air;
- $\gamma = 1$ volume occupied by water.

The nature of the VOF method means that an interface between the species is not explicitly computed, but rather emerges as a property of the phase fraction field. Since the phase fraction can have any value between 0 and 1, the interface is never sharply defined, but occupies a volume around the region where a sharp interface should exist.

Physical properties are calculated as weighted averages based on this fraction. The density ρ and viscosity μ in the domain are, therefore, calculated as follows:

$$\rho = \gamma\rho_1 + (1-\gamma)\rho_2 \tag{9}$$

$$\mu = \gamma\mu_1 + (1-\gamma)\mu_2 \tag{10}$$

where subscript 1 and 2 refer to the gas and the liquid, respectively.

Numerical diffusion will spread out the sharp interface between water and air. A compressive interface capturing scheme is used to re-sharpen the interface. Details about the present free surface modelling algorithm and the CICSAM scheme can be found in Ubbink and Issa (1999).

The VOF model has been designed for two or more immiscible fluids where only one fluid (i.e. air) is compressible and the position of the interface between the fluids is of interest. Therefore it is perfectly suitable for describing free-surface problems.

2.5 Numerical scheme for the three-dimensional approach

The model used in this work is based on an open source computational fluid dynamics (CFD) platform named OpenFOAM (OpenCFD, 2008), freely available on the Internet. OpenFOAM, primarily designed for problems in continuum mechanics, uses the tensorial approach and object oriented techniques (Weller et al., 1998). It provides a fundamental platform to write C++ new solvers for different problems as long as the problem can be written in tensorial partial differential equation form.

In this work, the high resolution VOF method proposed by Ubbink and Issa (1999) is used to track the free surface. The CICSAM (Compressive Interface Capturing Scheme for Arbitrary Meshes) scheme treats the whole domain as the mixture of two liquids. Volume fraction of each liquid is used as the weighting factor to get the mixture properties, such as density and viscosity.

The numerical solution of the Navier-Stokes equation for incompressible fluid flow imposes two main problems (Jasak, 1996): the nonlinearity of the momentum equation and the pressure-velocity coupling. For the first problem, two common methods can be used. The first is to solve a nonlinear algebraic system after the discretization. This will entail a lot of computational effort. The other is to linearize the convection term in the momentum equation by using the fluid velocity in previous time steps which meets the divergence-free condition. The latter method is used in this research. For pressure-velocity coupling, many schemes exist, such as the semi-implicit method for pressure linked equation (SIMPLE) (Patankar, 1981) and pressure implicit splitting of operators (PISO) (Issa, 1986). PISO scheme is used in this code. For the k-ε turbulence model equations, although k and ε equations are coupled together, they are solved with a segregated approach, which means they are solved one at a time. This is the approach used in most CFD codes.

3 Validation

The capabilities of the two models are here presented, comparing simulation results for two dam-break test cases:

1. partial instantaneous dam break over a flat bed without friction;
2. dam break flow over a triangular obstacle.

3.1 Test case 1: partial instantaneous dam break over flat bed without friction

The test consists in simulating the submersion wave due to the partial collapse of a dam. The spatial domain is a 200 m×200 m flat region, with a dam in the middle.

At the beginning of the simulation the water surface level is set in 10 m for the upstream region and 5 m for the downstream one. The unsteady flow studied in the present is generated by the instantaneous collapse of an asymmetrical 75 m long portion of the dam (barrier) (Fig. 1). The bottom is flat and ground resistance to the motion is neglected.

The aim of this validation is to study the capacity to simulate the front wave propagation, with particular attention to the two-dimensional and the three-dimensional aspects of the flow motion. As already pointed out, both methods use a square computational mesh with a spatial step of 5 m.

This test seems to be particularly suitable to highlight the differences between a shallow water approach and a full Navier-Stokes approach. Although there is no analytical reference solution for this test case, numerical results of various authors are available in literature (Fennema and Chaudhry, 1990; Alcrudo and Garcia-Navarro, 1993), as this test is usually considered a validation benchmark, as also reported in the CADAM project. However, even if the flow is three-dimensional, all the tests available in literature, as well as the results given by Fennema, typically used as the reference, have been carried out with simplified one- or two-dimensional models. In this paper the

three-dimensional effects, as well as their importance in terms of hydraulic design, are highlighted.

3.1.1 Simulations setup

Shallow water numerical model

The simulation with the shallow water model is carried out using a time step of 0.02 s. A null flow rate in the inlet section is set as the initial condition. All the computational domain is limited by no-slip walls.

Three-dimensional CFD numerical model

The test case was performed in a 200×200×20 m dominion. The geometric reconstruction was made through parametric meshes with grading and curved edges (Open Foam, 2008). The domain geometry is defined as a set of three dimensional, hexahedral blocks. Each block is defined by 8 vertices, one at each corner of a hexahedron. The computational mesh employed is a structured one with elementary volume entities of 5×5×1 m size.

The feature of the problem is a transient flow of two fluids separated by a sharp interface, or free surface. The solver is designed for two incompressible fluids capturing the interface by using the previously describe VOF method. Turbulence is modelled using a runtime selectable incompressible RANS model, with a standard k-ε model (Rodi, 1980) as closure equation. Figure 2 shows the initial and boundary conditions, by specifying the six patches.

The top boundary of the domain is the atmosphere and the total pressure is set to zero, all the others are set as wall, being the study case a closed box. The non-uniform initial condition for the phase fraction γ is specified.

3.1.2 Results

The computed water surface profiles were compared to Fennema numerical results (Fennema and Chaudhry, 1990), which was also obtained through a shallow water model solved with an implicit finite difference method. In particular, Fig. 3 shows the comparison of the computed water level 7.2 s after the breach, when the flow reached the left side of the tank.

The surface shape deriving from the shallow water model is in good agreement with the one obtained by Fennema (Alcrudo and Garcia-Navarro, 1993), except for a little delay in the front wave position. The level value is quite similar. This is an obvious consequence of the same shallow water schematization used. Significant differences are instead observed with the full Navier-Stokes three-dimensional model (Fig. 4):

- water surface levels immediately upstream the gate are lower than those predicted by the shallow water, due to the gravity force (Figs. 4 and 5);
- the front position shows that wave celerity is greater and water levels downstream the gate are higher than those predicted by the shallow water (Figs. 4 and 5).

These results agree with the conclusions drawn by De Maio et al. (2004), who observe that the shallow water model underestimates the front wave celerity and water depth profiles. This should be related to the three-dimensional aspects due to the gravity force, especially during the first time steps of the motion.

This behaviour is marked also in Fig. 6 where hydrographs at different monitor points are represented for both models.

The set of results originating from these simulations shows that the dam break problem is characterized by three-dimensional aspects, that have a great impact on water surface elevation and submersed wave travelling downstream.

The results demonstrated that 1-D models, traditionally used in hydraulic engineering, are not adequate to simulate the generation and propagation of the bore immediately after the gate failure (Morris and Galland, 2000). Therefore, these simplified

models should be coupled to detailed simulations of the dam break. Practically a detailed and a simplified one-dimensional model could be applied in cascade:

- simulation of the flood wave formation immediately after the collapse of the dam by means of a detailed model, in order to evaluate the discharge hydrograph,
- simulation of the propagation of this wave along the river by means of a hydraulic one-dimensional model (Werner, 2004) .

In order to evaluate when (at what instant after failure) and where (at what downstream cross section) it is possible to switch from a detailed to a one-dimensional model with sufficient accuracy, we extended the downstream domain up to 1000 m from the gate. A relevant parameter for this kind of study could be the water surface variation along cross section, defined as $h_{cv}=(h_{\max}-h_{\min})/h_0$.

Figure 7 shows water surface elevation and water surface variation along cross section at four different cross sections, located at a distance of 400, 500, 600 and 700 m from the gate, during the first 100 s after failure. The parameter $h_{cv}(t)$ could be used to establish a threshold value for the switch from the detailed to the simplified one-dimensional simulation. In other words, when the water surface variation along cross section is always lower than a certain value ($h_{cv}(t)\leq h_{cv,t}\forall t$), the approximation of a one-dimensional simulation could be acceptable. Setting this threshold to 10%, figure 7 highlights that a one-dimensional model could be used starting from a distance of 600 m from the gate (section E-E).

Figures 8 and 9 shows the difference in the water depth and the discharge hydrograph between the NS and the SW model at section E-E

Two aspects are relevant:

- SW model underestimates the peak flow of about 20% with respect to NS.
- the peak arrival time predicted by the SW model is higher than the correspondent three-dimensional one of about 4 s.

It is important to note that this shift time assumes a very important role in a real basin scale, as an incorrect prediction of the lead time may yield relevant errors in the emergency planning and risk mitigation activity.

3.2 Test case 2: dam break flow over a triangular obstacle

The second test case is an experimental dam break over a triangular obstacle performed at the Université Catholique de Louvain (UCL), in the laboratory of the Civil Engineering Department (Soarez-Frazao and Zech, 2002).

The experimental setup (Fig. 10) consists in a closed rectangular channel 5.6 m long and 0.5 m wide, with glass walls. The upstream reservoir extends over 2.39 m and is initially filled with 0.111 m of water at rest. The gate separating the reservoir from the channel can be pulled up rapidly in order to simulate an instantaneous dam break. Downstream from the gate, there is a symmetrical bump 0.065 high with a bed slope of 0.014. Downstream from the bump, a pool contains 0.025 m of water. It is thus a closed system where water flows between the two reservoirs and is reflected against the bump and against the upstream and downstream walls.

High-speed CCD cameras were used to film the flow through the glass walls of the channel at a rate of 40 images per second. The experiments show a good reproducibility, allowing to combine the images obtained from different experiments to form a continuous water profile (Fig. 11).

This test is almost two-dimensional in the plane x-z, but it can perfectly highlight the differences between the shallow water and the three-dimensional approach. It is, in fact, two-dimensional for the full Navier-Stokes model, but becomes one-dimensional for the shallow water model, as it neglects the elevation.

3.2.1 Simulation setup

Two-dimensional shallow water numerical model

The simulation was carried out using a spatial step of 0.05 m and a time step of 0.01 s. The computational mesh consists in 11×113 nodes. Figure 12 reports the initial condition schematization.

Three-dimensional CFD numerical model

The mesh geometry is composed by hexaedrons with 0.05 m side. The boundary patches are specified as wall, and atmosphere.

At wall surfaces (bed, flume walls, bump faces), no-slip boundary conditions are employed, that is to say u=0 is set for velocity with zero normal gradient for pressure. Surface tension effects between wall and water-air interface are neglected. This is done by setting the static contact angle, $\tilde{\theta}$=90° and the velocity scaling function to 0.

The top boundary of the domain is the atmosphere, where the total pressure is set to zero. For open boundaries the following conditions are applied: when the flow is going out of the domain, zero gradient condition is used, when the flow is entering the domain, a 1% turbulence intensity is used to specify k and epsilon. The small amount of air turbulence will not affect the water flow field too much since water is much heavier than air (Liu and García, 2008).

3.2.2 Results

The comparison between experimental and numerical results, with both models, is given in Fig. 13, in terms of free surface comparison at different times after the dam break.

During the collapse, the water impacts an obstacle at the bottom of the tank and creates a complicated flow structure, including several captured air pockets.

After the dam break, the water flows to the bump. Once it reaches this, a part of the wave is reflected and forms a negative bore travelling back in the upstream direction, while the other part moves up the obstacle (Fig. 13). At t=1.8 s (Fig. 13a), the shallow water model is not capable of reproducing the real situation: the front wave is not in agreement with the experimental data. The three-dimensional model simulation results are quite similar to real behaviour.

After passing the top of the bump, the water flows until it arrives in the second pool of water, where the front wave slows down and a positive bore forms (Fig. 13b, front-wave position=5.2 m). Again, the three-dimensional model results are in good agreement with the experimental data while the two-dimensional model is late.

At t=3.7 s (Fig. 13c), the bore has reflected against the downstream wall and is travelling back to the bump, but the water is unable to pass the crest. This behaviour is well reproduced by both models.

After a second reflection against the downstream wall, the wave has passed the bump and is travelling back into the upstream direction. Significant differences between the shallow water results and the experimental results are observable also at t=8.4 s (Fig. 13d).

The comparison between simulated and experimental results, given in Fig. 13, clearly shows that the three-dimensional model has the capability to represent the unsteady flow behaviour quite well. In fact, the flow picture frames captured at different times (top image at each time in Fig. 14) are all in good agreement with the numerical results (bottom image at each time in Fig. 14).

4 Conclusions

The present paper addresses a relevant problem in hydraulic engineering: the selection of an appropriate model to undertake dam break flood routing.

The type of flow model may be classified according to the number of spatial dimensions they simulate (1-D, two-dimensional, three-dimensional) the equations upon

which their predictions are based and the numerical system applied to solve these equations during the simulation process.

In the present paper, a three dimensional mathematical model has been applied for modelling dam break flows. The model has been validated by means of two test cases, a dam break over a flat bed without friction and a dam break over a triangular bottom sill. The results demonstrate that the formation of a dam-break wave is a fully three-dimensional phenomenon, which can be accurately simulated only by means of a full Navier Stokes model. Simplified shallow water and one-dimensional models underestimate the wave front celerity immediately after the gate collapse and do not reproduce the water depth profiles well. Also the flood wave speed is often poorly predicted.

The simulation of the partial instantaneous dam break over flat bed without friction emphasize relevant differences between the SW and the NS simulations. In particular the NS predicts lower water surface levels immediately upstream the gate and greater wave celerity and water levels downstream the gate. The differences are related to the three-dimensional effects of the gravity force, especially during the first time steps of the motion.

It is important to note that the above differences may assume a significant role in real world applications, as dam-break flood risk prone areas mapping and emergency planning. An underestimation of wave celerity and water levels, for example, means that the flood wave may arrive sooner and may be more destructive than what predicted.

The study of the dam break phenomenon also suggests the applications of a detailed and a hydraulic simplified models in cascade: simulation of the formation of the flood wave immediately after the collapse of the dam by means of a three-dimensional model, in order to evaluate the discharge hydrograph;simulation of the propagation of this wave along the river by means of a 1-D model.

The comparison between simulated and experimental results, performed for the second test case, clearly shows that the three-dimensional model has the capability to represent the unsteady flow behaviour quite well in the whole observation period, while

significant differences between experimental data and numerical results from the shallow water model are observed.

References

Abbott, M. B. and Basco, D. R.: Computational Fluid Dynamics: An Introduction for Engineers, Longman Scientific and Technical, Harlow, Essex, England, Wiley, New York, NY, 1989.

Alcrudo, F. and Soares Frazão, S.: Conclusions from 1st CADAM meeting, Proc. of 1st CADAM meeting, paper 5, HR Wallingford, Wallingford (UK), 1998.

Alcrudo, F. and Garcia-Navarro, P.: A high-resolution Godunov-type scheme in finite volumes for the two-dimensional shallow-water equations, Int. J. Numer. Meth. Fl., 16, 489–505, 1993.

Boussinesq, J.: Théorie Analytique de la Chaleur, Gauthier-Villars, Paris, 1903.

De Maio, A., Savi, F., and Sclafani, L: Three-dimensional mathematical simulation of dambreak flow, Proceeding of IASTED conferences – Environmental Modelling and Simulation, St. Thomas, US Virgin Island, ISBN 0-88986-441-1, 2004.

Faber, T. E.: Fluid Dynamics for Physicists, Cambridge University Press, Cambridge, UK, 1995.

Fennema, R. J. and Chaudhry, M. H.: Explicit methods for two-dimensional transient free-surface flows, J. Hydraul. Eng.-ASCE, 116(1), 1013–1034, 1990.

Galperin, B. and Orszag, S. A. (Eds.): Large Eddy Simulation of Complex Engineering and Geophysical Flows, Cambridge University Press, Cambridge, UK, 622 pp., 1993.

Hirsch, C.: Numerical Computation of Internal and External Flows, John Wiley and Sons, New York, 1992.

Issa, R. I.: Solution of the implicitly discretised fluid flow equations by operator-splitting, J. Comput. Phys., 62(1), 40–65, 1986.

Jasak, H. G.: Error Analysis and Estimation for the Finite Volume Method with Application to Fluid Flows, PhD thesis, Imperial College of Science, Technology and Medicine, London, UK, 1996.

Jorgenson, J., Xinya, Y., and Woodman, W.: Two-dimensional modeling of dam breach flooding, US–China workshop on advanced computational modelling in hydroscience and engineering, 19–21 September, Oxford, Mississippi, USA, 2004.

Jia, Y. and Wang, S. S. Y.: Numerical model for channel flow and morphological change studies, J. Hydraul. Eng-ASCE, 125, 924–933, 1999.

Jia, Y. and Wang, S. S. Y.: Two-Dimensional Hydrodynamic and Sediment Transport Model for Unsteady Open Channel Flow Over Loose Bed, 2001, Tech. Rep. NCCHE-TR2001-01, NCCHE, 2001.

Liu, X. and García, M. H.: A three-dimensional numerical model with free water surface and mesh deformation for local sediment scour, J. Waterw. Port. C.-ASCE, 134(4), 203–217, 2008.

Manciola, P., Mazzoni, A., and Savi, F.: Formation and Propagation of Steep Waves: An Investigative Experimental Interpretation, Proceedings of the Specialty Conference Co-sponsored by ASCE-CNR/CNDCI-ENEL spa held in Milan, Italy, 29 June–1 July 1994.

Mohammadi, M.: Boundary shear stress around bridge piers, Am. J. Appl. Sci., 5(11), 1546–1550, 2008.

Morris, M. W. and Galland, J. C.: Dam Break modelling Guidelines and Best Practice, Final Report CADAM concerted Action on dam break modelling, HR Wallingford, Wallingford, UK, 2000.

Nagata, N., Hosoda, T., Nakato, T., and Muramoto, Y.: Three-dimensional numerical model for flow and bed deformation around river hydraulic, J. Hydraul. Eng.-ASCE, 131, 1074–1087, 2005.

Open FOAM: The Open Source CFD Toolbox, User Guide, Version 1.5, 9 July 2008, OpenCFD, 2008.

Patankar, S. V.: Numerical Heat Transfer and Fluid Flow, McGraw-Hill, New York, USA, 1981.

Rodi, W.: Turbulence Models and Their Application in Hydraulics, International Association of Hydraulic Engineering (IAHR) Monograph, Delft, The Netherlands, 1980.

Soares Frazão, S.: Dam-break induced flows in complex topographies. Theoretical, numerical and experimental approaches, PhD Thesis, Università catholique de Louvain, Louvain-la-Neuve, Civil Engineering Department, Hydraulics Division, 116(1), 2002.

Soarez Frazão, S. and Zech, Y.: Dam break in channels with 90_ bend, J. Hydraul. Eng.-ASCE, 128(11), 956–968, 2002.

Ubbink, O. and Issa, R. I.: A method for capturing sharp fluid interfaces on arbitrary meshes, J. Comput. Phys., 153, 26–50, 1999.

Wang, J. S., Ni, H. G., and He, Y. S.: Finite-difference TVD scheme for computation of dam-break problems, J. Hydraul. Eng.-ASCE, 126(4), 253–261, 2000.

Wang, S. S. Y. and Hu, K. K.: Improved methodology for formulating finite-element hydrodynamic models, in: Finite Element in Fluids, Volume 8, edited by: Chung, T. J., Hemisphere

Publication Cooperation, Washington, DC, 457–478, 1992.
Weller, H. G., Tabor, G., Jasak, H., and Fureby, C.: A tensorial approach to computational continuum mechanics using object-oriented techniques, Comput. Phys., 12(6), 620–631, 1998.
Werner, M. G. F.: A comparison of flood extent modelling approaches through constraining uncertainties on gauge data, Hydrol. Earth Syst. Sci., 8, 1141–1152, 2004, http://www.hydrol-earth-syst-sci.net/8/1141/2004/.

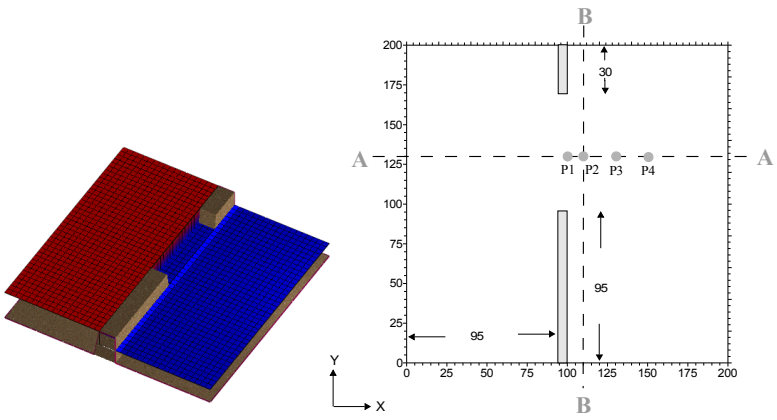

Fig. 1. Plan View (dimension in m) – geometric schematization of dam break over flat bed without friction test case. In plan, sections A-A B-B, points P1 (100,130), P2 (110,130), P3 (130,130), P4 (150,130) are shown.

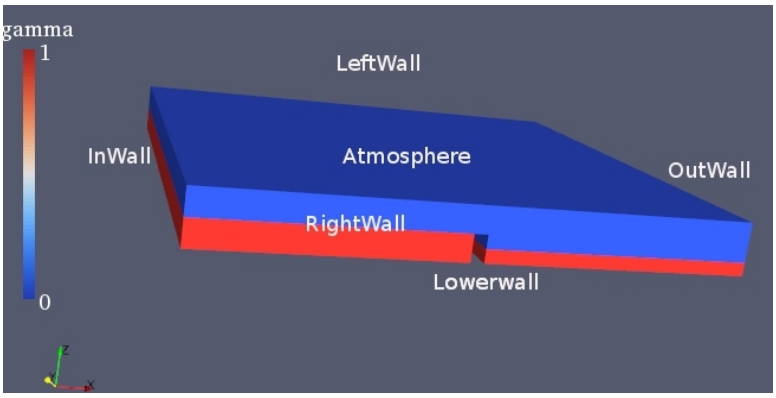

Fig. 2. Initial and boundary conditions. γ=0 gas phase only (blue), γ=1 liquid phase only (red).

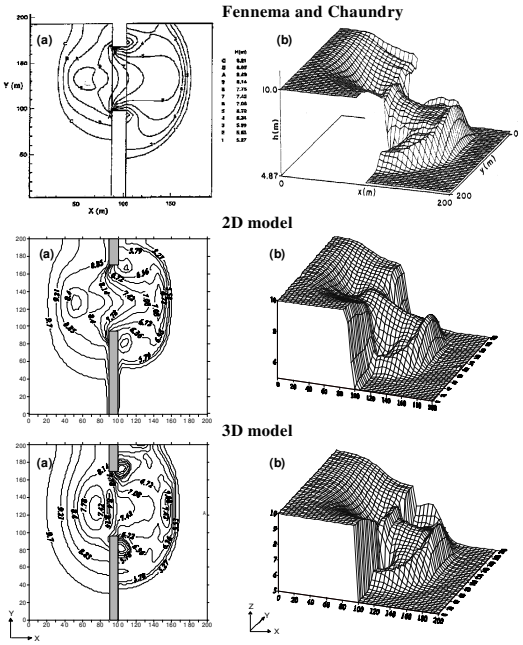

Fig. 3. Comparison between Fennema and Chaundry (1989), shallow water, full Navier Stokes simulations' results: (**a**) contour levels at 5.2, 5.7, 6.2, 6.7, 7.2, 7.8, 8.2, 8.7, 9.2 m. (**b**) Water surface wireframe (three-dimensionalview) after 7.2 s from failure.

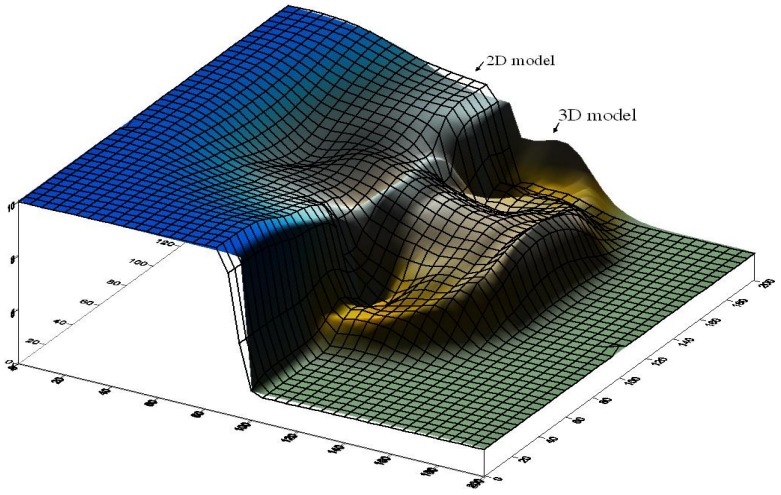

Fig. 4. Comparison of the water surface between the shallow water (grid) and the full Navier Stokes model (continuous contour).

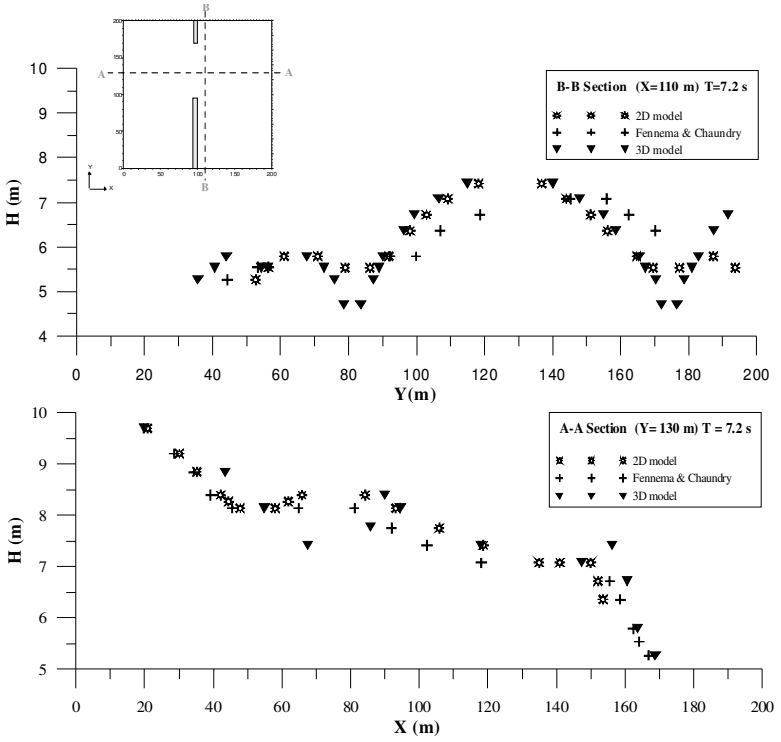

Fig. 5. Water depth at 7.2 s after the gate collapse: B-B and A-A sections.

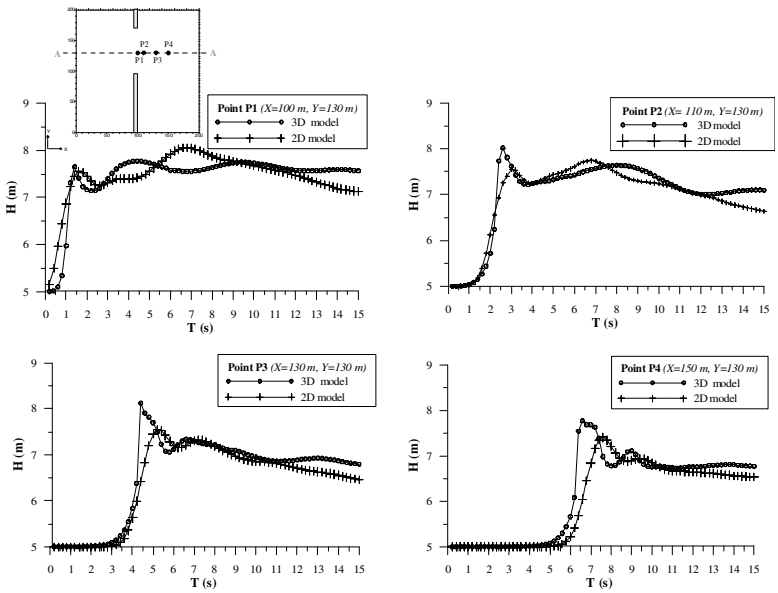

Fig. 6. Water level hydrograph at points P1, P2, P3, P4.

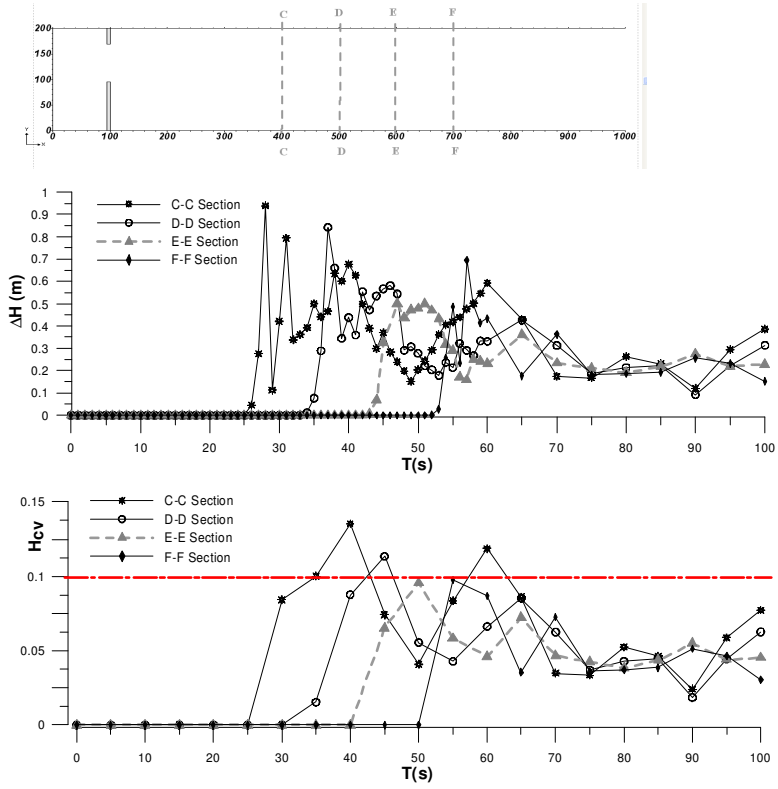

Fig. 7. Δh and h_{cv} depending on time at different cross section: C-C (x=400), D-D (x=500), E-E (x=600), F-F (x=700).

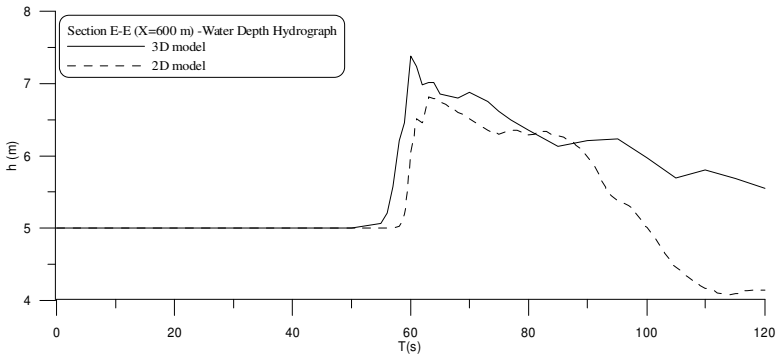

Fig. 8. Water depth hydrograph at E-E section (x=600).

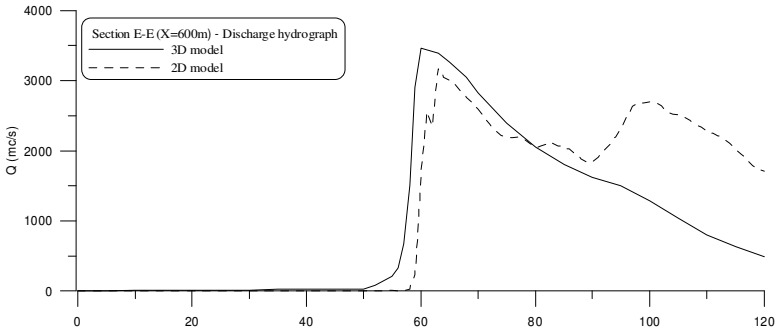

Fig. 9. Discharge hydrograph at E-E section (x=600).

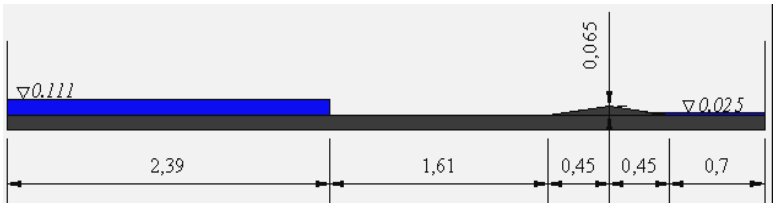

Fig. 10. Experimental set-up and initial conditions, all dimensions in m.

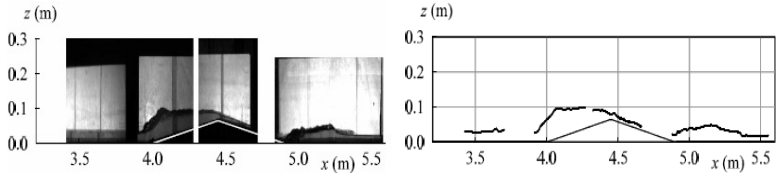

Fig. 11. Water surface at 1.8 s (Soaerez et al., 2002): the position of the free surface is measured by an automatic recognition procedure to each filmed image.

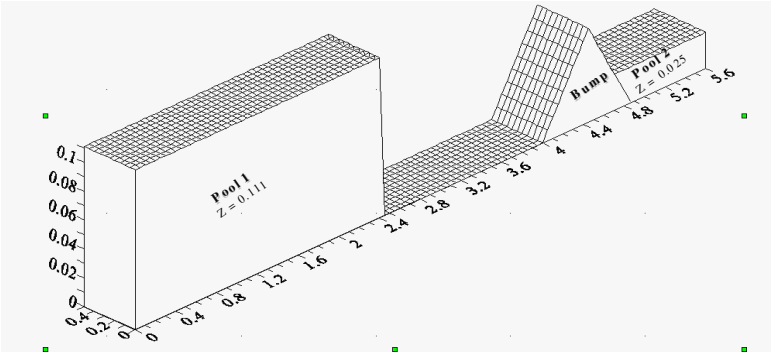

Fig. 12. Initial condition for the bump test case.

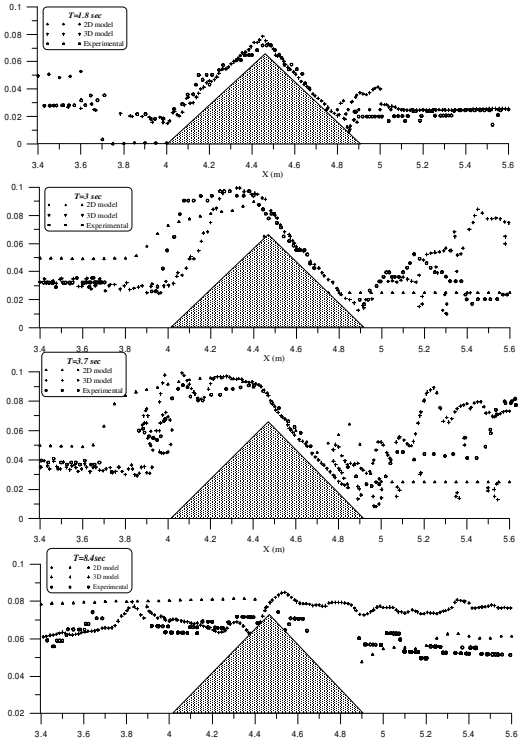

Fig. 13. Two-dimensional model, three-dimensional model, experimental water surface profile at T =1.8 s (**a**), T =3 s (**b**), T =3.7 s (**c**), T =8.4 s (**d**).

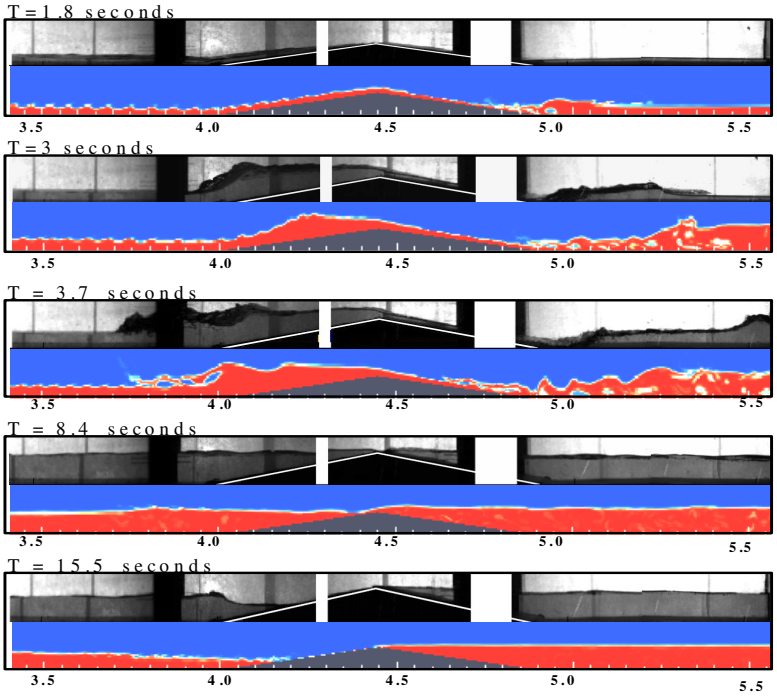

Fig. 14. Comparison between three-dimensional model results (bottom) and pictures of the experiment (top).